PAPER

Aggregation of an anionic porphyrin with chiral metal complexes and the competitive binding influences of a surfactant and a polyelectrolyte

Jian Wang,[a] Chengyong Liu,[b] Dongdong Ding,[b] Lixi Zeng,[a] Qian Cao,[a] Hui Zhang,*[b] Hong Zhao,*[a] Xiangjun Li,*[a] Kaixiang Xiang,*[c] Yujian He*[ad] and Guangwei Wang*[e]

The non-covalent interactions of chiral metal complexes with the achiral 5,10,15,20-tetrakis (4-sulonatophenyl) porphyrin (H_4TTPS^{2-}) have been investigated by UV-vis and circular dichroism (CD) spectra. The results show that under acidic environments, only the chiral complex cations ($[CoBr(NH_3)(en)_2]^+$, $[Co(en)_3]^{3+}$, $[Ru(phen)_3]^{2+}$) could interact with H_4TTPS^{2-} to form chiral aggregates, accompanied with the metal-centered chirality information transferred to the formed J-aggregates. However, the chiral complex anion ($[Co(edta)]^-$) does not cause the self-assembly process. The competitive binding interactions between an achiral water-soluble cationic surfactant (*N*-hexadecyltrimethyl ammonium chloride, CTAC) and a cationic polyelectrolyte (polyallylamine, PAA) with the chiral metal complex H_4TTPS^{2-} J-aggregates, respectively, were also investigated. It was found that chiral-symmetry-breaking phenomena occur in the cationic surfactant induced event. In the case of a cationic polyelectrolyte, it could change the conformational flexibility of the H_4TTPS^{2-} aggregates. These results may lead us to understand the possible mechanism of the supramolecular self-assembly process by the non-covalent interactions.

Introduction

Chirality is a central theme in nature, ranging from the molecular level to the supramolecular level, and from the microscopic to the macroscopic length scale.[1,2] The increasing interest in chiral supramolecular assemblies is not only to understand the origin of biomolecular homochirality, but also for their potential applications, such as molecular conductors,[3–8] chiral supramolecular liquid crystals,[9–16] chiroptical devices,[16–20] and other functional materials.[21–27] There are great interests concerning the transformation of chiral information from a chiral mold to achiral molecules and supramolecular systems. By forming intrinsically chiral assemblies, or by aggregating on to a chiral template, the symmetric

achiral molecules could also present supramolecular chirality. Construction of a chiral molecular assembly is very important in supramolecular chemistry. A number of researchers have revealed that some small achiral molecules can form chiral nano/micro-structures by host–guest and guest–guest interactions.[28–40] The driving force for the formation of chiral supermolecules is generally constructed on the non-covalent interactions, such as van der Waals interactions, hydrogen bonds, π–π stacking, metal coordination, electrostatic interaction and hydrophobic interactions.

Porphyrin derivatives play important roles in biological systems and spectroscopic studies for their novel and tunable spectroscopic, photophysical and photochemical properties.[41–47] Their unique planar as well as rigid molecular geometry and aromatic electronic feature delocalized over the molecular frame enable them to be well investigated in the field of constructing supramolecular assemblies by non-covalent interactions.[48–53] Various artificial photo-devices based on the chiral porphyrin supermolecules are anticipated to be potentially useful for the practical applications.[54–57]

In our previously reported work, we found that the random symmetry breaking in the synthesis of a chiral octahedral cobalt complex (*cis*-$[CoBr(NH_3)(en)_2]Br_2$) could be transferred in the supramolecular self-assembly process of anionic porphyrin derivatives.[58] What we are interested in is how did the chirality at the small molecular level transfer to the

[a] *College of Chemistry and Chemical Engineering, Graduate University of Chinese Academy of Sciences, Beijing 100049, China. E-mail: yujianhe@hotmail.com; hongzhao@gucas.ac.cn; lixiangj@gucas.ac.cn; Fax: +86 10-8825-6093; Tel: +86 10-8825-6141*
[b] *College of Chemistry and Chemical Engineering, Xiamen University, Xiamen 361005, China. E-mail: huizhang@xmu.edu.cn; Tel: +86 592-2183910*
[c] *Huaihua Medical College, Hunan, 418000, China. E-mail: hhyzggkb@163.com*
[d] *State Key Laboratory of Natural and Biomimetic Drugs, Peking University, Beijing 100083, China*
[e] *Medical College, Hunan Normal University, Changsha, Hunan 410006, China. E-mail: wanggwwmq323@163.com*

advanced supramolecular level. In this paper, we describe the interactions of the dye molecule of a porphyrin derivative (H_4TPPS^{2-}) with the chiral-only-at-metal complexes. Interestingly, we found that only the chiral complex cations could interact with H_4TTPS^{2-} to cause the self-assembly process, accompanied with their metal-centered chirality information transferred to the formed J-aggregates. The CD signals of the J-aggregates induced by the enantiomers are mirror-images. However, the chiral complex anion does not cause the self-aggregation process. We also systematically investigated the competitive binding events of the chiral H_4TPPS^{2-} J-aggregates with a water-soluble cationic surfactant (N-hexadecyltrimethyl ammonium chloride, CTAC) and a cationic polyelectrolyte (polyallylamine, PAA). The results show that the cationic surfactant can cause the formation of H_4TPPS^{2-} J-aggregates, and the formed J-aggregates show chirality due to chiral-symmetry-breaking. The handedness of the aggregates can be further guided by chiral metal complexes. In the case of a cationic polyelectrolyte, due to the short-ranged stacking of the porphyrins to the pyridinium residues after the addition of PAA, the conformational flexibility was changed. These results may lead us to gain more insights on the non-covalent interactions of the supermolecules.

Experimental section

1. Materials

The porphyrin derivative, 5,10,15,20-tetrakis(4-sulfonatophenyl)porphyrin (H_2TPPS^{4-}), was purchased from Fluka. The cetyltrimethylammonium chloride (CTAC, cationic surfactant) and the aqueous solution (20%) of poly(allylamine) (PAA, polycation electrolyte, average molecular weight, ca. 17 000) were purchased from Aldrich. Concentrated hydrochloric acid (HCl) was purchased from Beijing Chemical Co. All chemicals were used as received without further purification.

The chiral-only-at-metal complexes used in this work were synthesized according to the reported literature.[59–63]

2. Chiral assembly of the H_4TPPS^{2-} induced by different metal complexes

(1) Preparation of solutions. The stock solutions of the chiral-only-at-metal complexes (1 mM) were prepared by dissolving them in 0.01 M HCl solution (pH = 2.0).

10 mL solution of H_4TPPS^{2-} (10 μM) was freshly prepared by dissolving the H_2TPPS^{4-} crystal in distilled water at pH 2.0 that was adjusted by 0.1 M HCl solution.

(2) Chiral induction of the H_4TPPS^{2-}. The chiral-only-at-metal complexes were added to the solution of H_4TPPS^{2-} (10 μM, 10 mL) (pH = 2.0), respectively, to make metal complexes–porphyrin samples at a molar ratio 1 : 4 of H_4TPPS^{2-} : metal complex (4 μL, 0.01 M). These solutions were kept at room temperature overnight before characterization.

(3) The competitive binding of a cationic surfactant and a polycation electrolyte on the chiral H_4TPPS^{2-} J-aggregates. The chiral cobalt complex, [Co(en)₃]I₃·H₂O (4 μL, 0.01 M), was chosen as a chiral inducer in the self-aggregation process of H_4TPPS^{2-} (10 mL, 10 μM). After the mixture was

stabilized, different volumes of 2, 4, 6, 8, 10 μL CTAC (1 mmol L⁻¹) were added to the solutions, respectively. In another experiment, 2 μL CTAC (1 mmol L⁻¹) was firstly used to cause the formation of J-aggregates, and after the solution was stabilized, different volumes of 4, 6, 8, 10, 12 μL [Co(en)₃]I₃·H₂O (0.01 M) were added.

(4) The competitive binding of a polycation electrolyte on the chiral H_4TPPS^{2-} J-aggregates. Similar to the above experimental section, [Co(en)₃]I₃·H₂O (4 μL, 0.01 M) was firstly chosen as a chiral inducer in the self-aggregation process of H_4TPPS^{2-} (10 mL, 10 μM). After the mixture was stabilized overnight, different volumes of 2, 4, 6, 8, 10 μL PAA (1 g L⁻¹) were added to the solutions, respectively. In the opposite manner, 2 μL PAA (1 g L⁻¹) was firstly used to cause the formation of J-aggregates, and after the solution was stabilized, different volumes of 4, 6, 8, 10, 12 μL [Co(en)₃]I₃·H₂O (0.01 M) were added.

The above solutions were kept at room temperature overnight before characterization.

(5) Characterizations. The UV-vis adsorptions and CD spectra were measured (1 cm cell) using a UV-2550 spectrophotometer (Japan) and a Jasco J-810 spectropolarimeter (Japan), respectively. Fluorescence spectra were obtained on a LS 55 fluorescence spectrometer (Perkin-Elmer).

Results and discussions

1. Formation of H_4TPPS^{2-} J-aggregates induced by different chiral metal complexes

The structures of the four pairs of chiral-only-at-metal complexes and the porphyrin (H_4TPPS^{2-}) are shown in Fig. 1. All the chiral-only-at-metal complexes used have a quasi-octahedral structure.

The CD spectra of the four pairs of enantiomers are shown in Fig. 2. The CD spectra of the Λ-cis-[CoBr(NH₃)(en)₂]Br₂ ($\Delta\varepsilon_{564} = +0.333$) and Δ-cis-[CoBr(NH₃)(en)₂]Br₂ ($\Delta\varepsilon_{564} = -0.336$), Λ-[Co(en)₃]I₃·H₂O ($\Delta\varepsilon_{493} = +1.64$) and Δ-[Co(en)₃]I₃·H₂O ($\Delta\varepsilon_{493} = -1.52$), Λ-[Ru(phen)₃](PF₆)₂ ($\Delta\varepsilon_{268} = +352.99$) and Δ-[Ru(phen)₃](PF₆)₂ ($\Delta\varepsilon_{268} = -414.59$), Λ-K[Co(edta)]·2H₂O ($\Delta\varepsilon_{580} = +1.55$) and Δ-K[Co(edta)]·2H₂O ($\Delta\varepsilon_{580} = -1.61$) are approximately perfect mirror-images, respectively, and thus these complexes should be enantiomers of each other.

It is well-known that when the pH value is below 3, the pyrrole nitrogen atoms in the porphyrin cycle are diprotonated and a zwitterionic species is formed with a global −2 charge. The Soret band shifts from 412 to 434 nm and the Q bands become degenerated, which results in a change in the molecular symmetry from D_{2h} to D_{4h}.[64] The positively-charged center of the H_4TPPS^{2-} molecule can attract the negatively charged peripheral sulfonate groups of the adjacent H_4TPPS^{2-} molecules, resulting in edge-to-edge stacking.[65] Thus, the H_4TPPS^{2-} can be easily self-assembled to form J-aggregates at a low pH and/or at a high ionic strength atmosphere. The formation of porphyrin assemblies could be determined by the variation of the absorption and emission spectral properties. Aggregation of the monomer often leads to quite an extensive
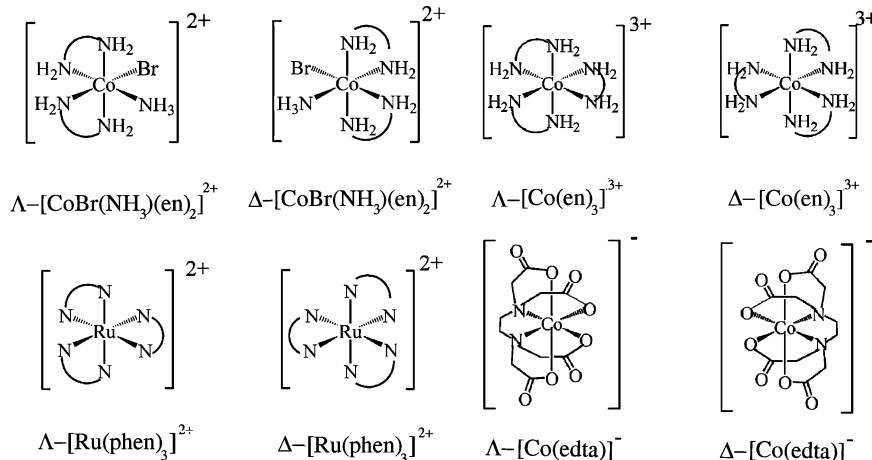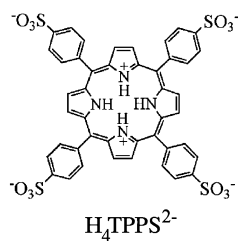
H_4TPPS^{2-}

$\Lambda-[CoBr(NH_3)(en)_2]^{2+}$ $\Delta-[CoBr(NH_3)(en)_2]^{2+}$ $\Lambda-[Co(en)_3]^{3+}$ $\Delta-[Co(en)_3]^{3+}$

$\Lambda-[Ru(phen)_3]^{2+}$ $\Delta-[Ru(phen)_3]^{2+}$ $\Lambda-[Co(edta)]^-$ $\Delta-[Co(edta)]^-$

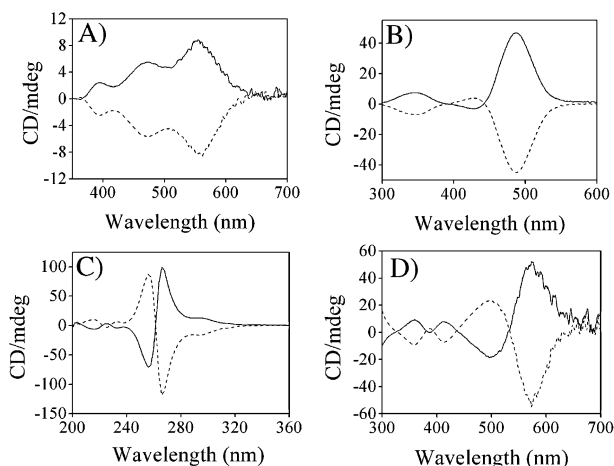**Fig. 1**   Schematic structures of H_4TPPS^{2-} and four pairs of chiral metal complexes.

Fig. 2   CD spectra of four pairs of chiral metal complexes. (A) cis-$[CoBr(NH_3)(en)_2]Br$; (B) $[Co(en)_3]I_3 \cdot H_2O$; (C) $[Ru(phen)_3](PF_6)_2$; (D) $K[Co(edta)] \cdot 2H_2O$ (solid line: Λ-configuration; dashed line: Δ-configuration).

Fig. 3   UV-vis spectra of the H_2TPPS (10 μM) after the addition of different metal complexes (solid line); (A) cis-$[CoBr(NH_3)(en)_2]Br$; (B) $[Co(en)_3]I_3 \cdot H_2O$; (C) $[Ru(phen)_3](PF_6)_2$; (D) $K[Co(edta)] \cdot 2H_2O$. (All dashed lines in the figure represent the absorbance of the H_4TPPS^{2-} without the addition of any metal complexes).

hypochromism of the Soret band and to a relevant, almost complete quenching of the porphyrin emission.[66]

Fig. 3 shows the change in UV-vis absorption spectra of the H_4TPPS^{2-} (10 μM) before and after the addition of the metal complexes. At pH = 2, the N atoms of the porphyrin cycle are diprotonated, which causes a red-shift of its Soret band to 434 nm. (All dashed lines in Fig. 3 represent the absorbance of the H_4TPPS^{2-} (10 μM) without the addition of any metal complexes, and the solid lines represent the absorbance of the H_4TPPS^{2-} (10 μM) after the addition of the four metal complexes). In Fig. 3A–C, obviously, we can see that after
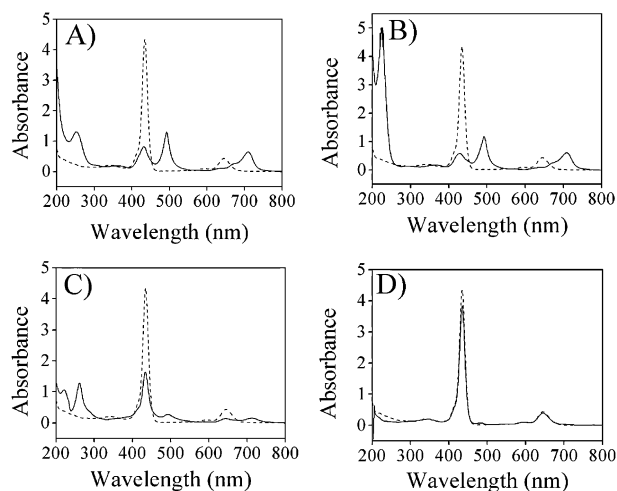
the addition of the complex (Fig. 3A: $[CoBr(NH_3)(en)_2]^+$; Fig. 3B: $[Co(en)_3]^{3+}$; Fig. 3C: $[Ru(phen)_3]^{2+}$), the characteristic absorption of the monomer at 434 nm decreased, and a new absorption at 491 nm appeared, which was the characteristic absorption of the edge-to-edge H_4TPPS^{2-} J-aggregates. However, there was no obvious change in the UV-vis spectrum of the H_4TPPS^{2-} monomer after the addition of the complex anion of $[Co(edta)]^-$ (Fig. 3D). It indicated that the porphyrin molecules existed in the monomeric form, $i.e.$ the $[Co(edta)]^-$

complex cannot induce the formation of H_4TPPS^{2-} J-aggregates.

2. Circular dichroism of H_4TPPS^{2-} J-aggregates induced by different chiral-only-at-metal complexes

The interaction between the chiral inorganic cationic complex and H_4TPPS^{2-} was further confirmed by the appearance of an induced CD signal in the absorption region of porphyrins. As shown in Fig. 4, after the addition of chiral complex cations, the chiral-at-metal information could be transmitted to the H_4TPPS^{2-} J-aggregates. In Fig. 4A, the chiral J-aggregates induced by Λ-[CoBr(NH$_3$)(en)$_2$]$^+$ show a negative Cotton effect at 488 nm, 415 nm and a positive signal at 502 nm. In Fig. 4B, the Λ-[Co(en)$_3$]$^{3+}$ could lead to a quite different spectroscopic behavior, that is two positive Cotton effects at 482 nm, 411 nm and two negative signals at 488 nm and 508 nm. In Fig. 4C, the Λ-[Ru(phen)$_3$]$^{2+}$ caused two negative Cotton effects at 490 nm, 414 nm and two negative signals at 481 nm and 422 nm. The CD signals of the chiral H_4TPPS^{2-} J-aggregates induced by the enantiomers of the above metal complexes show mirror-image signals. This pattern of splitting Cotton effect suggested the existence of exciton coupling between the porphyrin chromophores due to the aggregation of the diprotonated species.[67] In one word, the CD signals of
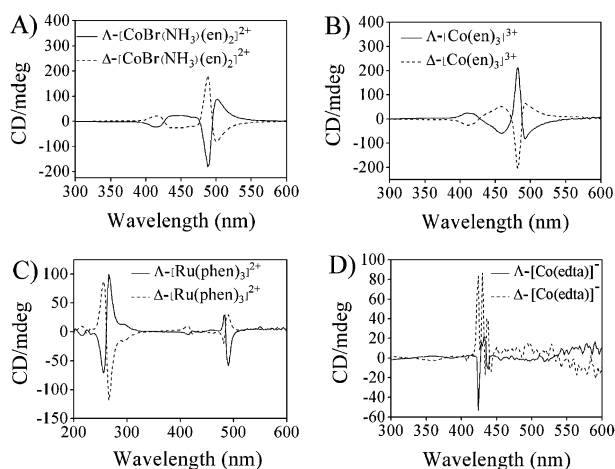
the H_4TPPS^{2-} J-aggregates depend on the absolute configuration of the chiral metal complexes, and the sign of the ICD follows the chirality of the inorganic metal complex templates.

However, because it could not cause the self-assembly process after the addition of [Co(edta)]$^-$, no obvious spectral change around 482 nm is observed (Fig. 4D).

3. Fluorescence study of the H_4TPPS^{2-} J-aggregates induced by different chiral-only-at-metal complexes

Fluorescence spectra are successively measured under the same aforementioned experimental systems. The effect of the cobalt complexes on the fluorescence spectra for 10 μM H_4TPPS^{2-} is monitored at different excitation wavelengths (434 nm, 491 nm). As shown in Fig. 5A, under excitation at 434 nm, the fluorescence of the H_4TPPS^{2-} monomer (line a) and H_4TPPS^{2-} in the presence of K[Co(edta)]·2H$_2$O (line b) showed a peak at 668 nm. However, the addition of [Co(en)$_3$]I$_3$·H$_2$O (line c), [CoBr(NH$_3$)(en)$_2$]Br (line d) and [Ru(phen)$_3$](PF$_6$)$_2$ (line e) to the H_4TPPS^{2-} resulted in the hypsochromic shift of the main fluorescence peak to about 660 nm.

While being excited at the wavelength of 491 nm (Fig. 5B), the main peak of the fluorescence emission spectra of the H_4TPPS^{2-} monomer and H_4TPPS^{2-} in the presence of K[Co(edta)]·2H$_2$O appeared at 668 nm. However, their intensity became lower compared to that excited at the wavelength of 434 nm. While in the presence of [Co(en)$_3$]I$_3$·H$_2$O, [CoBr(NH$_3$)(en)$_2$]Br and [Ru(phen)$_3$](PF$_6$)$_2$, the peak became wider together with its position shifted to about 655 nm. However, while being excited at 491 nm, the characteristic emission peak of the J-band was not observed at 714 nm. It is expected that quenching happened in the emission spectra of the formed H_2TPPS^{4-} J-aggregates. This quenching phenomenon could also demonstrate that there is a strong interaction between the H_4TPPS^{2-} and the metal complexes.

4. The effect of water-soluble cationic surfactant on the chiral H_4TPPS^{2-} J-aggregates

According to the previously reported literature, the water soluble cationic surfactant (cetyltrimethylammonium chloride, CTAC) can also cause the self-aggregation of monomer H_4TPPS^{2-} to form J-aggregates and H-aggregates at different conditions.[68,69]

Fig. 4 CD spectra of the H$_2$TPPS (10 μM) after the addition of different metal complexes; (A) Δ-/Λ-cis-[CoBr(NH$_3$)(en)$_2$]Br; (B) Δ-/Λ-[Co(en)$_3$]I$_3$·H$_2$O; (C) Δ-/Λ-[Ru(phen)$_3$](PF$_6$)$_2$; (D) Δ-/Λ-K[Co(edta)]·2H$_2$O.
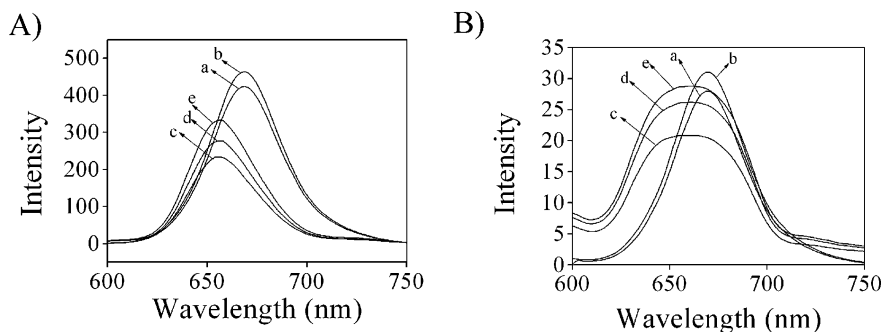

Fig. 5 Fluorescence spectra of H$_4$TPPS^{2-} in the presence of different chiral metal complexes. (A) λ_{ex} = 434 nm; (B) λ_{ex} = 490 nm. (a: H$_4$TPPS^{2-} without any metal complexes; b: K[Co(edta)]·2H$_2$O; c: [Co(en)$_3$]I$_3$·H$_2$O; d: cis-[CoBr(NH$_3$)(en)$_2$]Br; e: [Ru(phen)$_3$](PF$_6$)$_2$).

Fig. 6 (A) UV-vis spectrum of the H_4TPPS^{2-} J-aggregate induced by Λ-[Co(en)$_3$]$^{3+}$ (40 μM) (dashed line) and after the addition of different amounts of CTAC (solid line) (inset: change in UV-absorbance t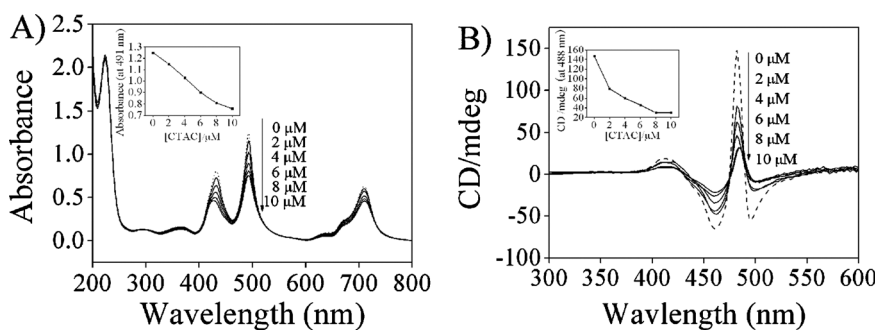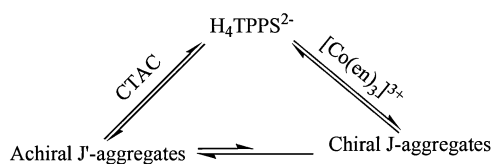owards the addition of the concentration of CTAC); (B) CD spectrum of the H_4TPPS^{2-} J-aggregate induced by Λ-[Co(en)$_3$]$^{3+}$ (40 μM) (dashed line) and after the addition of different amounts of CTAC (solid line) (inset: CD intensity change towards the addition of the concentration of CTAC).

To investigate the effect of the positively charged surfactant on the chiral H_4TPPS^{2-} J-aggregates, competitive binding events between CTAC and metal complexes with the H_4TPPS^{2-} J-aggregates were conducted. We choose Λ-[Co(en)$_3$]$^{3+}$ as a chiral cationic inducer to guide the formation of chiral H_4TPPS^{2-} J-aggregates. In this experiment, the chiral H_4TPPS^{2-} J-aggregates were firstly formed by the addition of chiral metal complexes, and after they stabilized, CTAC with different concentrations was titrated with the solution. The changes of UV-vis absorbances and CD spectra after the addition of CTAC are shown in Fig. 6.

UV-vis absorbance in Fig. 6A shows that the addition of CTAC does not cause any peak shift in both the characteristic Soret band (434 nm) and the Q band (491 nm) of J-aggregates. However, the absorption intensity at the Soret band decreased with increasing the CTAC concentration, and this indicated that the free monomer H_4TPPS^{2-} was further induced to form new J-aggregates. It was worth to note that the absorption intensity at the Q band (491 nm) also decreased with increasing the CTAC concentration, this meant that the chiral H_4TPPS^{2-} J-aggregate formed by the induction of Λ-[Co(en)$_3$]$^{3+}$ was degraded. It indicated that the J-aggregates with CTAC (denoted as J$'$-aggregates) should be more stable than the H_4TPPS^{2-} J-aggregate with Λ-[Co(en)$_3$]$^{3+}$ (denoted as J-aggregates) in the system (Scheme 1).

The CD data in Fig. 6B show that the CD signal of the chiral H_4TPPS^{2-} J-aggregates around 488 nm gradually decreased with the increase of CTAC concentration, and there was a red-shift from 488 to 490 nm. This further indicated that the racemic J$'$-aggregates with CTAC were formed, and the chiral H_4TPPS^{2-} J-aggregate with Λ-[Co(en)$_3$]$^{3+}$ was degraded. In this process, the cationic surfactant CTAC may competitively bind to free H_4TPPS^{2-} to form the racemic

H_4TPPS^{2-} aggregates, and decrease the CD singal of the chiral aggregates.

It is worth to note that when the concentration of CTAC is up to 8 μM, the further addition of CTAC does not cause any change of the CD intensity at 490 nm. This indicated that the H_4TPPS^{2-} monomer, J$'$-aggregates with CTAC and the chiral J-aggregate with Λ-[Co(en)$_3$]$^{3+}$ reached an equilibrium, and the J$'$-aggregates with CTAC may be dominated to result in a red-shift from 488 to 490 nm.

Then we conducted the experiment in an opposite manner, that is the J$'$-aggregates were firstly formed by the induction of CTAC (2 μM), and after stabilizing, a chiral cobalt complex Λ-[Co(en)$_3$]$^{3+}$ with different concentrations was titrated to the system.

The changes of UV-vis absorbances and CD spectra after the addition of CTAC are shown in Fig. 7A and B. From Fig. 7A, it is obviously observed that the addition of chiral Λ-[Co(en)$_3$]$^{3+}$ caused an intensity decrease in the Soret band (434 nm) and increase in the Q band (489 nm), which demonstrated that left J-aggregates with Λ-[Co(en)$_3$]$^{3+}$ were formed.

Interestingly, when we measured the circular dichroism(CD) spectra of the H_4TPPS^{2-} J-aggregates which were induced by CTAC, we observed a clear Cotton effect at 488 nm although there is no chiral molecule in the solution, as shown in Fig. 7B. It is further observed that the CD signal was relatively weak and the sign of the Cotton effect could be opposite in different experimental batches. This suggested that chiral symmetry breaking occurred during the self-assembly process.[70] Once the J-aggregate formed, a mixture of left- and right-handed aggregates formed. However, these two chiral species might not be equally generated and one of them would be in excess and then amplified during the growth of the J-aggregate. Therefore, we observed the CD signal for H_4TPPS^{2-} J-aggregates induced by the CTAC.

If a chiral species, for example, Δ-, or Λ-[Co(en)$_3$]$^{3+}$, was added in the mixed solvents, the handedness of the formed H_4TPPS^{2-} J-aggregates was found to be controlled. Fig. 7B showed that the CD intensity of the H_4TPPS^{2-} J-aggregates increased with increasing the concentration of the chiral Λ-[Co(en)$_3$]$^{3+}$. This clearly indicated that in the presence Λ-[Co(en)$_3$]$^{3+}$, the chirality of the H_4TPPS^{2-} J-aggregates followed the "chiral sergeant". When we used Δ-[Co(en)$_3$]$^{3+}$ in the solution, the mirror-image CD spectrum was obtained (data not shown).

Scheme 1 Schematic illustration of the competitive binding events of chiral H_4TPPS^{2-} J-aggregates with Λ-[Co(en)$_3$]$^{3+}$ and achiral H_4TPPS^{2-} J$'$-aggregates with CTAC.
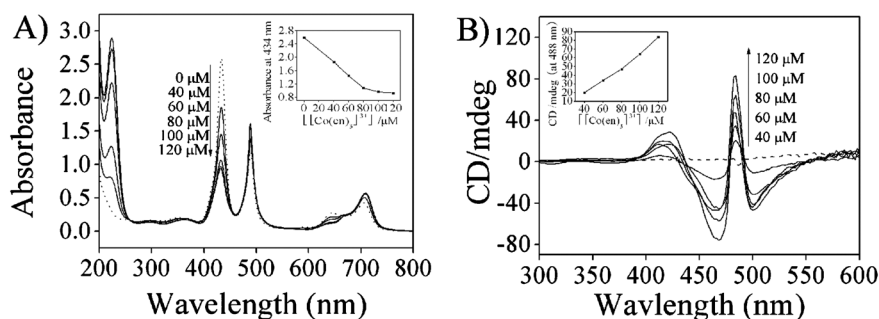
Fig. 7 (A) UV-vis spectrum of the H_4TPPS^{2-} J-aggregate induced by CTCA (2 μM) (dashed line) and after the addition of different amounts of Λ-$[Co(en)_3]^{3+}$ (solid line) (inset: change in UV-absorbance towards the addition of the concentration of Λ-$[Co(en)_3]^{3+}$); (B) CD spectrum of the H_4TPPS^{2-} J-aggregate induced by CTCA (2 μM) (dashed line) and after the addition of different amounts of Λ-$[Co(en)_3]^{3+}$ (solid line) (inset: change in CD intensity towards the addition of the concentration of Λ-$[Co(en)_3]^{3+}$).

5. The effect of polycation in H_4TPPS^{2-} J-aggregates formation

Polycation (poly(allyamine), PAA) could also be used to cause the self-assembly of H_4TPPS^{2-}.[71] Around pH 7, the H_4TPPS^{2-} could be assembled into H-aggregates that are aligned perpendicularly to the line connecting neighboring molecules in the aggregates.[72] While around pH 1, PAA is protonated, due to the strong electrostatic interaction between the positively charged PAA and the anionic H_4TPPS^{2-} bearing four negatively-charged sulfonate residues on the mesophenyl substitutes group, PAA could interact with H_4TPPS^{2-} to form a J-aggregate whose monomer units stacked as in a slipped deck of cards.

The changes in UV-vis spectra after the addition of PAA are shown in Fig. 8A and B.

Fig. 8A shows the UV-vis spectrum of the H_4TPPS^{2-} J-aggregate induced by Λ-$[Co(en)_3]^{3+}$ and after the addition of different amounts of PAA. The absorption intensity at 434 nm decreased with increasing the PAA concentration, this indicated that the free monomer H_4TPPS^{2-} was induced to form new J-aggregates. And, the absorption intensity at the Q-band (491 nm) also decreased with increasing the PAA concentration, this meant that the chiral H_4TPPS^{2-} J-aggregate formed by the induction of Λ-$[Co(en)_3]^{3+}$ was degraded. It was worth to note that the Soret band at 434 nm of the diprotonated H_4TPPS^{2-} was shifted to 424 nm when the

concentration of PAA is up to 6 μg mL^{-1}. This shift of the monomer band of the H_4TPPS^{2-} has been found while short-range interactions are held with the surrounding species because of dipole interactions with the transition moments.[73–76] However, the position of the characteristic spectrum of the J-aggregated H_4TPPS^{2-} at 491 nm does not shift, suggesting the existence of J-aggregates.

The CD data in Fig. 8B show that the CD signal of the chiral H_4TPPS^{2-} J-aggregates around 488 nm gradually decreased with the increase of PAA concentration, but no shift of the peak position was found in the PAA event. This is due to the conformational flexibility change through the competitive binding event between Λ-$[Co(en)_3]^{3+}$–H_4TPPS^{2-} J-aggregates and PAA–H_4TPPS^{2-} aggregates.

Among many non-covalent interactions, including the π–π force, electrostatic force, hydrogen bonding and charge-transfer interactions for the formation of highly ordered J-aggregates of H_4TPPS^{2-}, the π–π force is dominantly important over the others. While a relatively low concentration of PAA was added to the system, it competed with $[Co(en)_3]^{3+}$ for binding to the sites ($-SO^{3-}$) of the formed chiral H_4TPPS^{2-} J-aggregates and replaced the $[Co(en)_3]^{3+}$ by the multiple-point electrostatic interaction. The flexible PAA can easily combine with the chiral H_4TPPS^{2-} J-aggregates and twist along the helical direction, forming the advanced stiff H_4TPPS^{2}–PAA complex. When more PAA was added, the π–π force in the porphyrin J-aggregates is broken down
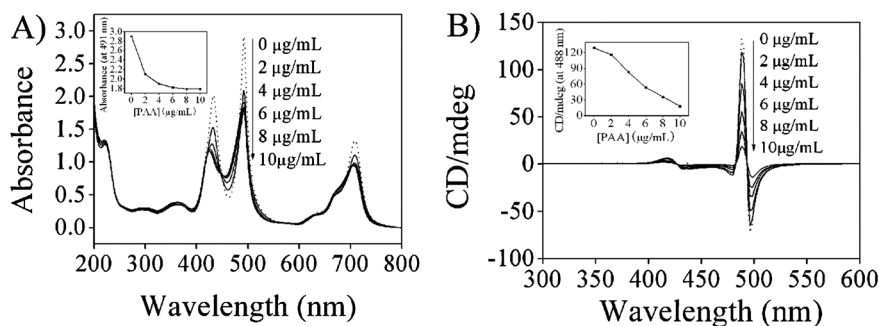

Fig. 8 (A) UV-vis spectrum of the H_4TPPS^{2-} J-aggregate induced by Λ-$[Co(en)_3]^{3+}$ (40 μM) (dashed line) and after the addition of different amounts of PAA (solid line) (inset: change in UV-absorbance towards the addition of the concentration of PAA); (B) CD spectrum of the H_4TPPS^{2-} J-aggregate induced by Λ-$[Co(en)_3]^{3+}$ (40 μM) (dashed line) and after the addition of different amounts of PAA (solid line) (inset: change in UV-absorbance towards the addition of the concentration of PAA).
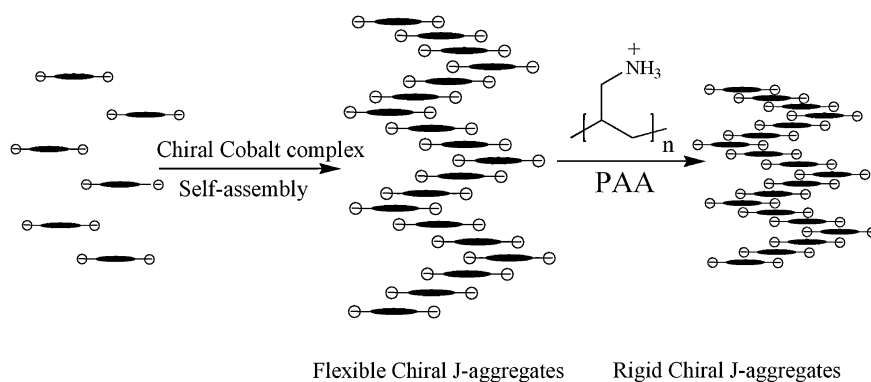
Scheme 2 Schematic illustration of the chiral H_4TPPS^{2-} J-aggregate from flexible to rigid after the addition of a polyelectrolyte.

by the electrostatic force, and the short-ranged electrostatic force between the positively charged PAA and the anionic H_4TPPS^{2-} became dominant, so the Soret band of H_4TPPS^{2-} at 434 nm shifted to 424 nm, and more condensed J-aggregates were formed by this short-ranged electrostatic force (Scheme 2).

If the J-aggregates were firstly induced by PAA ($2\ \mu g\ mL^{-1}$), the following addition of the cobalt complex does not cause peak shift in the UV-vis spectra. As seen in Fig. 9A, the J-aggregates induced by PAA ($2\ \mu g\ mL^{-1}$) have their characterized absorbance at 434 nm and 490 nm. The following addition of the cobalt complexes causes the absorbance decrease at 434 nm, and no obvious change was observed at 490 nm. The CD spectrum was also taken to characterize the H_4TPPS^{2-}–PAA aggregates, as show in Fig. 9B, no ICD signal was detected of the PAA induced H_4TPPS^{2-} J-aggregates. However, the addition of the chiral cobalt complexes could cause a bisignated Cotton effect at 498 nm and 488 nm. The intensity increased with more chiral cobalt complexes added. It is worth to note that the CD intensity of the H_4TPPS^{2-}–PAA aggregates followed by $[Co(en)_3]^{3+}$ is relatively smaller compared to the $[Co(en)_3]^{3+}$ induced H_4TPPS^{2-} J-aggregates. This is because PAA is an achiral scaffold to guide the assembling process of H_4TPPS^{2-}, the following addition of the chiral inducer could only partly twist the flexibility.

We then use PAA with a high concentration ($6\ \mu g\ mL^{-1}$) to induce the self-assembly of H_4TPPS^{2-}. The UV-vis spectra are shown in Fig. 10, at high concentration of PAA, the characteristic absorbance of J-aggregates at 490 nm coexists with an absorption band at 424 nm. According to the reported literature, the absorption band at 424 nm has the shape of the monomer bands, and this shift of the monomer bands from 434 nm to 424 nm is explained by the stacking of the porphyrins to the pyridinium residues which caused a short-range interaction among the surrounding species. We then add the chiral $[Co(en)_3]^{3+}$ to the solution, but no peak shift was found (dashed line). When we measured the CD spectra, however, there is no CD signal of the J-aggregates after the addition of chiral $[Co(en)_3]^{3+}$ (data not shown). This is because the high concentration of PAA causes the self-assembly of H_4TPPS^{2-} to form more compressed and rigid J-aggregates, the following $[Co(en)_3]^{3+}$ could not twist the flexibility, thus the stiff structure of H_4TPPS^{2-}–PAA J-aggregates keeps achiral.

6. Possible mechanism of the interactions of the anionic porphyrin with the metal complex

Shi and his co-workers reported that in the acidic aqueous solution, the copolymer PEG_{114}-*b*-$P(4VP)_{38}$ could turn into a typical neutral–cationic double hydrophilic block copolymer (DHBC), and result in the protonation of the P(4VP) blocks. By the electrostatic attraction between the $4(VPH)^+$ block of the PEG_{114}-*b*-$P(4VPH^+)_{38}$ and the $-SO_3^-$ group of the TPPS, micelles with an ion-complex of $P(4VPH^+)$ and TPPS as the core and a water-soluble PEG block as the shell could be
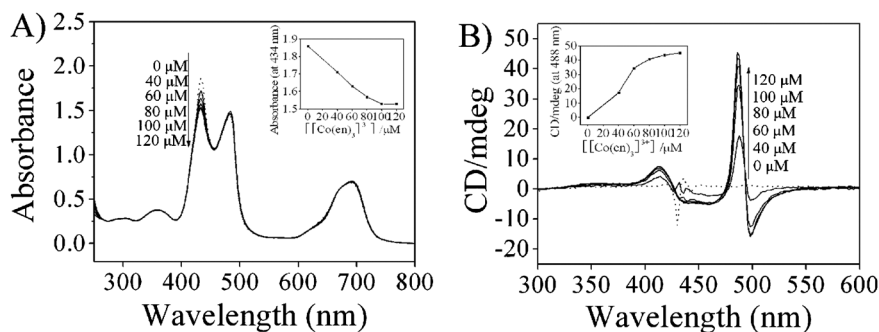

Fig. 9 (A) UV-vis spectrum of the H_4TPPS^{2-} J-aggregate induced by PAA ($2\ \mu g\ mL^{-1}$) (dashed line) and after the addition of different amounts of Λ-$[Co(en)_3]^{3+}$ (solid line) (inset: change in UV-absorbance towards the addition of the concentration of Λ-$[Co(en)_3]^{3+}$); (B) CD spectrum of the H_4TPPS^{2-} J-aggregate induced by PAA ($2\ \mu g\ mL^{-1}$) (dashed line) and after the addition of different amounts of Λ-$[Co(en)_3]^{3+}$ (solid line) (inset: change in CD intensity towards the addition of the concentration of Λ-$[Co(en)_3]^{3+}$).
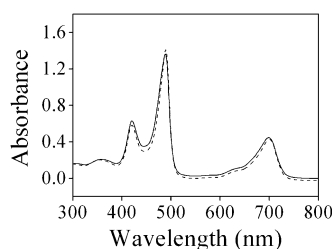
Fig. 10 UV-vis spectrum of the H_4TPPS^{2-} J-aggregate induced by PAA (6 µg mL^{-1}) (dashed line) and after the addition of Λ-[Co(en)$_3$]$^{3+}$ (solid line).

formed.[77] Liu *et al.* reported the chiral self-assembly of the anionic porphyrin in the presence of chiral cationic polymers such as poly(L-lysine) (PLL) or poly(D-lysine) (PDL) by the electrostatic attractive interaction.[78] In one of our previous work we found that under a low pH condition, the protonated amino groups of various amino acids could also transfer their chiral information to the anionic H_4TPPS^{2-} supramolecular aggregates. The possible mechanism is based on the chiral amino acids binding to porphyrins through electrostatic interactions between the positively charged amino cations of amino acids and the negatively charged sulfonato anions of a porphyrin.[39] Other works related to the self-assembly of porphyrin derivatives also showed that the electrostatic force dominated in the formation of porphyrin J-aggregates.[79,80]

According to the reported literature and our experimental results, we can speculate that the interaction of the metal complex with the H_4TPPS^{2-} may be *via* also an electrostatic interaction mechanism. At pH = 2, the protonated species of H_4TPPS^{2-} is zwitterionic, and the supramolecular processes are dominated by the electrostatic interactions and π–π stacking among the porphyrin monomers. The positively charged complex of [CoBr(NH$_3$)(en)$_2$]$^{2+}$, [Co(en)$_3$]$^{3+}$ and [Ru(phen)$_3$]$^{2+}$ could serve as a center of condensation due to partial neutralization of approaching H_4TPPS^{2-} molecules, thus helping them to come into closer contact with each other and lead to the transformation of the chirality to the J-aggregates. For the electrostatic repulsion effect between the complex anion ([Co(edta)]$^-$) and negatively charged sulfonate groups, the distance among the porphyrin monomers increased, making them far from each other, so it is difficult to cause the self-aggregation behavior.[81] The above competitive binding events between the cationic surfactant and polyelectrolyte with the chiral metal complex further demonstrate the mechanism of the electrostatic effect on the chiral self-assembly process.

We have also investigated the effect of the chiral metal complexes on the self-assembly process of the cationic pseudoisocyanine (PIC). The preliminary experimental results show that only the multiple π-conjugated chiral metal complexes could transfer their chiral information to the cationic PIC J-aggregates. That indicated the driving force of the chiral induced process in the cationic monomer PIC is dominated by the π–π stacking between the PIC monomer and the multiple π-conjugated metal complexes. This interesting work is still being investigated in our lab. These works may help us to understand the mechanism in the self-organization processes.

Conclusions

In summary, we have investigated the non-covalent interaction between the achiral well extended π-conjugate dye molecules (H_4TPPS^{2-}) and four pairs of chiral metal complexes. The interaction is primarily based on the intramolecular π–π stacking and the intermolecular electrostatic force. The results showed that only chiral complex cations of [Co(en)$_3$]$^{3+}$, [CoBr(NH$_3$)(en)$_2$]$^+$ and [Ru(phen)$_3$]$^{2+}$ could induce the self-assembly of the anionic porphyrin derivatives, with their chirality transferred to the formed J-aggregates. The competitive binding events of the H_4TPPS^{2-}–cobalt complex with a cationic surfactant and a polycation electrolyte have also been investigated. The CTAC induced J-aggregates show chirality due to chiral-symmetry-breaking. The helicity of the aggregates can be further controlled by chiral additives. It was also found that the polycation electrolyte (PAA) could competitively bind to the H_4TPPS^{2-}–cobalt J-aggregates, and make the J-aggregates more compressed and stiff. These results can help us understand the mechanism of non-covalent interactions in the self-assembly process of the chiral supermolecules.

Acknowledgements

References

1 R. Purrello, *Nat. Mater.*, 2003, **2**, 216.
2 R. Lauceri and R. Purrello, *Supramol. Chem.*, 2005, **17**, 61.
3 C. Rethore, N. Avarvari, E. Canadell, P. Auban-Senzier and M. Fourmigue, *J. Am. Chem. Soc.*, 2005, **127**, 5748.
4 J. D. Wallis and J. P. Griffiths, *J. Mater. Chem.*, 2005, **15**, 347.
5 J. Sly, P. Kasak, E. Gomar-Nadal, C. Rovira, L. Gorriz, P. Thordarson, D. B. Amabilino, A. E. Rowan and R. J. M. Nolte, *Chem. Commun.*, 2005, 1255.
6 M. Kimura, S. Otsuji, J. Takizawa, Y. Tatewaki, T. Fukawa and H. Shirai, *Chem. Lett.*, 2010, 812.
7 H. Goto, Y. Okamoto and E. Yashima, *Chem.–Eur. J.*, 2002, **8**, 4027.
8 T. Hatano, A. H. Bae, M. Takeuchi, N. Fujita, K. Kaneko, H. Ihara, M. Takafuji and S. Shinkai, *Angew. Chem., Int. Ed.*, 2004, **43**, 465.
9 P. Iavicoli, H. Xu, L. N. Feldborg, M. Linares, M. Paradinas, S. Stafstrom, C. Ocal, B. L. Nieto-Ortega, J. Casado, J. T. L. Navarrete, R. Lazzaroni, S. De Feyter and D. B. Amabilino, *J. Am. Chem. Soc.*, 2010, **132**, 9350.
10 A. J. Soininen, E. Kasemi, A. D. Schluter, O. Ikkala, J. Ruokolainen and R. Mezzenga, *J. Am. Chem. Soc.*, 2010, **132**, 10882.
11 N. Gimeno, M. J. Clemente, P. Forcen, J. L. Serrano and M. B. Ros, *New J. Chem.*, 2009, **33**, 2007.
12 M. van Houtem, R. Martin-Rapun, J. Vekemans and E. W. Meijer, *Chem.–Eur. J.*, 2010, **16**, 2258.
13 L. de Vega, P. D. Ortiz, G. Hennrich, A. Omenat, R. M. Tejedor, J. Barbera, B. Gomez-Lor and J. L. Serrano, *J. Phys. Chem. B*, 2010, **114**, 4811.

14 E. Beltran, E. Cavero, J. Barbera, J. L. Serrano, A. Elduque and R. Gimenez, *Chem.–Eur. J.*, 2009, **15**, 9017.
15 J. del Barrio, R. M. Tejedor, L. S. Chinelatto, C. Sanchez, M. Pinol and L. Oriol, *J. Mater. Chem.*, 2009, **19**, 4922.
16 J. Barbera, L. Giorgini, F. Paris, E. Salatelli, R. M. Tejedor and L. Angiolini, *Chem.–Eur. J.*, 2008, **14**, 11209.
17 J. del Barrio, R. M. Tejedor, L. S. Chinelatto, C. Sanchez, M. Pinol and L. Oriol, *Chem. Mater.*, 2010, **22**, 1714.
18 G. Zou, H. Jiang, Q. J. Zhang, H. Kohn, T. Manaka and M. Iwamoto, *J. Mater. Chem.*, 2010, **20**, 285.
19 G. C. Zhang and M. H. Liu, *J. Mater. Chem.*, 2009, **19**, 1471.
20 Y. F. Qiu, P. L. Chen, P. Z. Guo, Y. G. Li and M. H. Liu, *Adv. Mater.*, 2008, **20**, 2908.
21 Y. Z. Zhang, Z. M. Wang and S. Gao, *Inorg. Chem.*, 2006, **45**, 10404.
22 G. Rikken and E. Raupach, *Nature*, 1997, **390**, 493.
23 A. Mallick, S. Saha, P. Pachfule, S. Roy and R. Banerjee, *J. Mater. Chem.*, 2010, **20**, 9073.
24 K. L. Woon, M. O'Neill, G. J. Richards, M. P. Aldred, S. M. Kelly and A. M. Fox, *Adv. Mater.*, 2003, **15**, 1555.
25 J. Misek, A. V. Jentzsch, S. I. Sakurai, D. Emery, J. Mareda and S. Matile, *Angew. Chem., Int. Ed.*, 2010, **49**, 7680.
26 J. Jiang, T. Wang and M. H. Liu, *Chem. Commun.*, 2010, **46**, 7178.
27 S. S. Hu, J. Y. Li, J. F. Xiang, J. Pan, S. Z. Luo and J. P. Cheng, *J. Am. Chem. Soc.*, 2010, **132**, 7216.
28 O. K. Kim, J. Je, G. Jernigan, L. Buckley and D. Whitten, *J. Am. Chem. Soc.*, 2006, **128**, 510.
29 Y. Z. Zhang, J. F. Xiang, Y. L. Tang, G. Z. Xu and W. P. Yan, *ChemPhysChem*, 2007, **8**, 224.
30 L. Stryer and E. R. Blout, *J. Am. Chem. Soc.*, 1961, **83**, 1411.
31 T. D. Slavnova, H. Gorner and A. K. Chibisov, *J. Phys. Chem. B*, 2007, **111**, 10023.
32 M. M. Wang, G. L. Silva and B. A. Armitage, *J. Am. Chem. Soc.*, 2000, **122**, 9977.
33 R. A. Garoff, E. A. Litzinger, R. E. Connor, I. Fishman and B. A. Armitage, *Langmuir*, 2002, **18**, 6330.
34 L. X. Zeng, Y. J. He, Z. F. Dai, J. Wang, C. Q. Wang and Y. G. Yang, *Sci. China, Ser. B*, 2009, **52**, 1227.
35 R. F. Pasternack, A. Giannetto, P. Pagano and E. J. Gibbs, *J. Am. Chem. Soc.*, 1991, **113**, 7799.
36 R. Purrello, A. Raudino, L. M. Scolaro, A. Loisi, E. Bellacchio and R. Lauceri, *J. Phys. Chem. B*, 2000, **104**, 10900.
37 S. Ikeda, T. Nezu and G. Ebert, *Biopolymers*, 1991, **31**, 12573.
38 A. S. R. Koti and N. Periasamy, *Chem. Mater.*, 2003, **15**, 369.
39 L. X. Zeng, Y. J. He, Z. F. Dai, J. Wang, Q. Cao and Y. L. Zhang, *ChemPhysChem*, 2009, **10**, 954.
40 L. Z. Zhao, X. Wang, Y. Li, R. J. Ma, Y. L. An and L. Q. Shi, *Macromolecules*, 2009, **42**, 6253.
41 P. Zhang, M. Wang, C. X. Li, X. Q. Li, J. F. Dong and L. C. Sun, *Chem. Commun.*, 2010, **46**, 8806.
42 H. B. Fa, W. Yin, C. J. Hou, W. Q. Zheng, D. J. Wang and X. Q. Wang, *J. Coord. Chem.*, 2009, **62**, 1151.
43 F. D'Souza, R. Chitta, S. Gadde, M. E. Zandler, A. L. McCarty, A. S. D. Sandanayaka, Y. Araki and O. Ito, *Chem.–Eur. J.*, 2005, **11**, 4416.
44 M. Gervaldo, P. A. Liddell, G. Kodis, B. J. Brennan, C. R. Johnson, J. W. Bridgewater, A. L. Moore, T. A. Moore and D. Gust, *Photochem. Photobiol. Sci.*, 2010, **9**, 890.
45 Y. S. Nam, T. Shin, H. Park, A. P. Magyar, K. Choi, G. Fantner, K. A. Nelson and A. M. Belcher, *J. Am. Chem. Soc.*, 2010, **132**, 1462.
46 S. Funyu, T. Isobe, S. Takagi, D. A. Tryk and H. Inoue, *J. Am. Chem. Soc.*, 2003, **125**, 5734.
47 N. Bennett, G. Z. Xu, L. J. Esdaile, H. L. Anderson, J. E. Macdonald and M. Elliott, *Small*, 2010, **6**, 2604.
48 A. Romeo, M. A. Castriciano and L. M. Scolaro, *J. Porphyrins Phthalocyanines*, 2010, **14**, 713.
49 Y. Q. Zhang, P. L. Chen and M. H. Liu, *Chem.–Eur. J.*, 2008, **14**, 1793.
50 Y. Q. Zhang, P. L. Chen, Y. P. Ma, S. G. He and M. H. Liu, *ACS Appl. Mater. Interfaces*, 2009, **1**, 2036.
51 M. Fathalla, A. Neuberger, S.-C. Li, R. Schmehl, U. Diebold and J. Jayawickramarajah, *J. Am. Chem. Soc.*, 2010, **132**, 9966.
52 M. Takeuchi, S. Tanaka and S. Shinkai, *Chem. Commun.*, 2005, 5539.
53 J. Mohanty, A. C. Bhasikuttan, S. D. Choudhury and H. Pal, *J. Phys. Chem. B*, 2008, **112**, 10782.
54 W. W. H. Wong, T. Khoury, D. Vak, C. Yan, D. J. Jones, M. J. Crossley and A. B. Holmes, *J. Mater. Chem.*, 2010, **20**, 7005.
55 H. Imahori, A. Fujimoto, S. Kang, H. Hotta, K. Yoshida, T. Umeyama, Y. Matano, S. Isoda, M. Isosomppi, N. V. Tkachenko and H. Lemmetyinen, *Chem.–Eur. J.*, 2005, **11**, 7265.
56 H. Ozawa, M. Kawao, S. Uno, K. Nakazato, H. Tanaka and T. Ogawa, *J. Mater. Chem.*, 2009, **19**, 8307.
57 B. Liao, R. G. Liu and Y. Huang, *Polym. J. (Tokyo)*, 2007, **39**, 1071.
58 J. A. Wang, D. D. Ding, L. X. Zeng, Q. A. Cao, Y. J. He and H. Zhang, *New J. Chem.*, 2010, **34**, 1394.
59 K. Asakura, K. Kobayashi, Y. Mizusawa, T. Ozawa, S. Osanai and S. Yoshikawa, *Physica D*, 1995, **84**, 72.
60 A. Werner, *Chem. Ber.*, 1911, **44**, 1887.
61 A. Werner, *Chem. Ber.*, 1912, **45**, 121.
62 F. P. Dwyer, E. C. Gyarfas and D. P. Mellor, *J. Phys. Chem.*, 1955, **59**, 296.
63 K. A. McGee and K. R. Mann, *J. Am. Chem. Soc.*, 2009, **131**, 1896.
64 P. M. R. Paulo and S. M. B. Costa, *Photochem. Photobiol. Sci.*, 2003, **2**, 597.
65 J. Valanciunaite, S. Bagdonas, G. Streckyte and R. Rotomskis, *Photochem. Photobiol. Sci.*, 2006, **5**, 381.
66 A. Mammana, M. De Napoli, R. Lauceri and R. Purrello, *Bioorg. Med. Chem.*, 2005, **13**, 5159.
67 Y. Q. Zhang, P. L. Chen and M. H. Liu, *Chem.–Eur. J.*, 2008, **14**, 1793.
68 N. C. Maiti, S. Mazumdar and N. Periasamy, *J. Phys. Chem. B*, 1998, **102**, 1528.
69 P. S. Santiago, D. D. Neto, L. R. S. Barbosa, R. Itri and M. Tabak, *J. Colloid Interface Sci.*, 2007, **316**, 730.
70 S. G. Jiang, L. Zhang and M. H. Liu, *Chem. Commun.*, 2009, 6252.
71 Y. Egawa, R. Hayashida and J. I. Anzai, *Langmuir*, 2007, **23**, 13146.
72 P. Kubat, K. Lang, P. Jandaa and P. Anzenbacher, *Langmuir*, 2005, **21**, 9714.
73 I. Moreno-Villoslada, T. Murakami and H. Nishide, *Biomacro-molecules*, 2009, **10**, 3341.
74 A. S. R. Koti and N. Periasamy, *J. Mater. Chem.*, 2002, **12**, 2312.
75 I. Moreno-Villoslada, F. Gonzalez, L. Arias, J. M. Villatoro, R. Ugarte, S. Hess and H. Nishide, *Dyes Pigm.*, 2009, **82**, 401.
76 Q. X. Wan, Y. Liu and S. S. Wang, *Monatsh. Chem.*, 2009, **140**, 335.
77 J. B. Li, Y. L. An, X. Chen, D. A. Xiong, Y. Li, N. Huang and L. Q. Shi, *Macromol. Rapid Commun.*, 2008, **29**, 214.
78 L. Zhang and M. H. Liu, *J. Phys. Chem. B*, 2009, **113**, 1405.
79 M. Urbanova, V. Setnicka, V. Kral and K. Volka, *Biopolymers*, 2001, **60**, 307.
80 X. D. Chen and M. H. Liu, *J. Inorg. Biochem.*, 2003, **94**, 106.
81 J. Valanciunaite, V. Poderys, S. Bagdonas, R. Rotomskis and A. Selskis, *J. Phys.: Conf. Ser.*, 2007, **61**, 1207.

This journal is © The Royal Society of Chemistry and the Centre National de la Recherche Scientifique 2011